



Impact of Nonlinear Rosseland Approximation on Flow of Newtonian Fluid with Unequal Diffusivities of Chemically Reactive Species

M. Sheikh¹ · Z. Abbas² · J. Hasnain³ · A. Nadeem⁴ · M. Sajid⁵

Received: 14 August 2020 / Accepted: 7 December 2020 / Published online: 6 January 2021
© King Fahd University of Petroleum & Minerals 2021

Abstract

This investigation studies the flow of a Newtonian fluid close to stagnation point past a stretching/shrinking plate embedded in a porous media. Heat transfer analysis with nonlinear thermal radiation (TR) is also carried out. Homogeneous-heterogeneous reactions with unequal diffusivities of reactants take place in the fluid. The controlling partial differential equations (DEs) of the existing model are reduced to dimensionless ordinary DEs through similarity transformations. These subsequent equations are numerically tackled with the guide of the shooting procedure. The velocity, temperature and concentration's behaviour has been inspected for specific estimations of the including parameters. The viscous fluid (VF) temperature increases with nonlinear TR. The change in the concentration profile due to the diffusion coefficient rate δ is more prominent in the concentration of specie D compared to specie C. Heterogeneous reaction parameter intensity is very helpful in reducing the concentration of bulk fluid $\phi_1(\eta)$ as well as increasing the surface catalyst concentration $\phi_2(\eta)$

Keywords Viscous fluid · Chemically reactive species · Nonlinear thermal radiation · Unequal diffusivity of species C and D.

List of Symbols

x, y Spatial coordinates [m]
 q_r Thermal radiation
 u, v Velocity components in x and y directions, [ms⁻¹]

Greek Symbols

p Pressure [kgm⁻¹s⁻²]
 ρ Density [kgm⁻³]
 c, d Concentrations of species C and D
 θ Temperature [K]
 $k_i (i = e, s)$ Rate constants

θ_w, θ_∞ Wall and free stream temperatures [K]
 q_r Thermal radiation
 ζ Permeability of porous zone
 k Thermal conductivity [Wm⁻¹K⁻¹]
 ν Kinematic viscosity [m²s⁻¹]
 C_p Specific heat capacity [Jkg⁻¹K⁻¹]
 σ^* Stephen Boltzmann constant
 D_C^*, D_D^* Diffusion coefficients
 ψ Stream function
 U_w, U_∞ Surface and free stream velocities [ms⁻¹]
 η dimensionless variable [-]
 k^* Wall mean absorption
 Θ_w Temperature ratio [-]
 K_s Heterogeneous reaction strength
 β Porosity parameter [-]
 Sc_C, Sc_D Schmidt numbers [-]
 λ Stretching/shrinking parameter [-]
 K Homogenous reaction strength
 δ Ratio of diffusion coefficients [-]
 Rd Radiation parameter [-]
 Θ Dimensionless fluid temperature [-]
 Pr Prandtl number [-]
 ϕ_1, ϕ_2 Dimensionless concentrations [-]
 f, f' Dimensionless velocities [-]

✉ J. Hasnain
jafar_hasnain14@yahoo.com

¹ Department of Mathematics, University of Sialkot, Sialkot 51310, Pakistan

² Department of Mathematics, The Islamia University of Bahawalpur, Bahawalpur 63100, Pakistan

³ Department of Computer Sciences, Bahria University, Islamabad 44000, Pakistan

⁴ Department of Mathematical Sciences, Federal Urdu University of Art, Science and Technology, Islamabad 44000, Pakistan

⁵ Department of Mathematics and Statistics, International Islamic University Islamabad, Islamabad 44000, Pakistan



1 Introduction

Boundary layer flow due to a stretchable surface is essential as it is beneficial in many application and engineering processes, i.e. extrusion produced materials, melt-spinning, wire drawing, manufacture of plastics, hot rolling, production of glass fibre, extrusion process, in production of polymer sheets and the association of biological fluids. BL flow in two dimensions for a viscous, laminar, as well as incompressible fluid due to a stretchable flat plate was first studied by Crane [1]. The liquid flowed at a speed that was proportional to a distance from a fixed point. Parhi and Nath [2] discussed the stability of BL flow of viscous liquid past a stretching plate. Kumaran et al. [3] examined the transition consequence of the magnetic field on the flow of VF due to a stretched wall. Yirga and Tesfay [4] numerically inspected the magnetohydrodynamic (MHD) flow of VF over an expanded wall. Hassan [5] applied the Lie group method to analyse the heat transfer on VF influenced by the magnetic field over an expanding surface. Sheikh and Abbas [6] looked into the consequence of thermophoresis on MHD flow of Newtonian liquid having chemically reactive species with heat transmission over an oscillatory stretched wall. Sigh et al. [7] explored the effects of nonlinear MHD on the flow of viscous fluid over a porous stretchable sheet with mass transpiration. Reddy and Reddy [8] dealt with heat and mass characteristics on BL flow of a VF because of an exponential inclined stretching sheet. On the other hand, Wang [9] first studied the problem in the reverse case, i.e. the flow caused by the shrinking sheet. In this article, he discussed the flow of a fluid over a shrinking sheet near stagnant point where the speed of a fluid is zero. Lok et al. [10] considered stagnant point flow of a Newtonian fluid past a contracting/expanding sheet and also discussed the existence and multiplicity of solutions of the flow. Rosila and Ishak [11] performed an analysis for SP flow in the presence of porous media past a SS sheet and obtained numerical results. By applying partial velocity slip and Joule heating, Yasin et al. [12] considered the VF flow in the vicinity of stagnant point. Nasir et al. [13] numerically examined the viscous liquid flow near SP past a quadratically SS plate. By considering viscous dissipation along with magnetic field effects, Alarifi et al. [14] studied the flow of VF past a vertical stretching sheet near SP.

Effects of thermal radiation (TR) on heat and mass transfer fluid have many significant practical applications, for example in solar power technology, electric power generator, space vehicle re-entry, radioactive waste disposal, chemical pollutants dispersal by water-saturated soil and much more. Many authors studied linear and nonlinear heat radiation effects. By using linear Rosseland

approximation (RA), Magyari and Pantokratoras [15] studied heat transfer features of different BL flows. Later, Pantokratoras [16] investigated the flow along the vertical plate by considering both linear and nonlinear RA. Laxmi and Shanker [17] considered the VF flow caused by a stretching sheet with nonlinear TR and suction/injection. The effects of thermal radiation on Carreau-Yasuda nanofluid in the presence of chemical reactions were discussed by Waqas et al. [18], and it was observed that thermal radiation raises Carreau-Yasuda nanofluid temperature. Raiz et al. [19] studied the heat transfer through the rectangular channel of the Eyring–Powell fluid flow. Hashim et al. [20] presented the numerical investigation of non-Newtonian fluid flow with nonlinear TR and nanoparticles. Pattnaik et al. [21] conducted a heat transfer study of nanofluid flow and found that when nanofluid was considered, there was a rapid decline in the temperature profile. Zhang et al. [22] looked at the influence of heat transfer with generalized magnetic Reynold number on the 3D nanofluid flow and observed that with the increase in the squeeze Reynolds number, temperature drops significantly.

Chemical reactions may be categorized as heterogeneous or homogeneous. This classification is based upon the occurrence of reactions whether the reactions happen at a single-phase volume reaction or they happen at a boundary. Food processing, development and diffusion of fog, design of chemical managing equipment, moisture above agricultural fields and fruit tree groves are some areas of concern where joined mass and heat transfer occurs with a chemical reaction. Various chemical reacting structures possess both heterogeneous as well as homogeneous reactions. The interaction between both reactions happening on some catalytic surfaces is exceptionally complicated, which could be integrated at different rates in the manufacturing as well as usage of reactant species either inside the fluid or on catalytic surfaces. Chaudhary and Merkin [23, 24] originally formulated a basic HH reactions model in the BL flow near SP. The case of unequal diffusivities of homogeneous-heterogeneous reactions in viscoelastic fluid flow with magnetic field and nonlinear thermal radiation was studied by Animasaun et al. [25] and reached to the result that the change due to δ in concentration profile is more noticeable for concentration of specie B relative to the specie A. Sheikh and Abbas [26] considered SP flow of non-Newtonian fluid with HH reactions along with slip effects. Alghamdi [27] explores the viscoelastic fluid flow with HH reactions exposed to the magnetic field.

The majority of flow and thermal transport phenomena are fundamentally nonlinear, so they are expressed by nonlinear equations. Accurate closed-form solutions to nonlinear problems are far more challenging to achieve than numerical ones. Researchers use several closed-form schemes and numerical schemes to figure out the solution



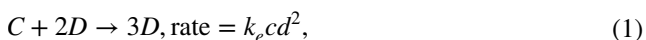
to the problems of the fluid flow under consideration. See references [28–33] for information.

Furthermore, in hydrometallurgical industries and chemical technologies such as polymer manufacturing and food processing, the chemical reaction effects on heat and mass transfer with radiation through porous media are of significant importance. See references. [34–43]

A porous medium means a material composed of a solid matrix with interconnected empty spaces. These interlinked spaces permit the flow of at least one fluid through the material. Composite materials, metallic foams with high porosity and ceramics are some common examples of porous media. Due to its natural occurrence and relevance in many engineering problems such as porous rollers, porous bearings, porous layer insulation consisting of solids and pores, and in biomathematics, especially in the study of blood flow in arteries and lungs, etc., considerable interest has been shown in the study of flow past a porous medium. Role of radiative heat transmission is superficial in many engineering processes which occur at high temperatures such as in photochemical reactors, turbid water bodies, fluidized bed heat exchangers, nuclear power plants and the various propulsion devices. It is worth noting in all the above literature that little attention has been paid to investigate the movement of a viscous fluid with unequal diffusivities of chemical reactions. So, the purpose of the present study is to examine the behaviour of BL flow of VF containing two chemically reactive species through porous media. This study also includes the effects of nonlinear TR, and here diffusion coefficients of both auto-catalyst and reactant are assumed to be unequal.

2 Governing Equation

On a stretchable surface near a SP, a steady BL flow is considered in the presence of porous medium and TR. Additionally, the sheet’s temperature along with the temperature at free stream are assumed as θ_w and θ_∞ , respectively, with $\theta_w > \theta_\infty$. A basic HH reactions model is also taken, which links the species C and D in a BL flow as described by [23] and [24]:



Furthermore, both reactive processes are supposed to be isothermal and a homogeneous concentration c_0 of reactant C is in the free stream and no auto-catalyst D is present.

The governing equations of the present flow situation, in the light of above presumptions and BL approximations, are given below [11, 25]

$$\frac{\partial u}{\partial x} + \frac{\partial v}{\partial y} = 0, \tag{3}$$

$$u \frac{\partial u}{\partial x} + v \frac{\partial u}{\partial y} = -\frac{1}{\rho} \frac{\partial p}{\partial x} + \nu \frac{\partial^2 u}{\partial y^2} - \frac{\nu}{\zeta} u, \tag{4}$$

$$u \frac{\partial \theta}{\partial x} + v \frac{\partial \theta}{\partial y} = \frac{k}{\rho C_p} \frac{\partial^2 \theta}{\partial y^2} - \frac{1}{\rho C_p} \frac{\partial q_r}{\partial y}, \tag{5}$$

$$u \frac{\partial c}{\partial x} + v \frac{\partial c}{\partial y} = D_C^* \frac{\partial^2 c}{\partial y^2} - k_e c d^2, \tag{6}$$

$$u \frac{\partial d}{\partial x} + v \frac{\partial d}{\partial y} = D_D^* \frac{\partial^2 d}{\partial y^2} + k_e c d^2. \tag{7}$$

The constraints at the surface of the sheet and away from it in the free stream are specified by (Fig. 1)

$$u = u_w(x) = U_w x, v = 0, \theta = \theta_w, D_C^* \frac{\partial c}{\partial y} = k_s c, D_D^* \frac{\partial d}{\partial y} = -k_s c \text{ at } y = 0, \tag{8}$$

$$u = u_\infty(x) = U_\infty x, \theta = \theta_\infty, c \rightarrow c_0, d \rightarrow 0 \text{ as } y \rightarrow \infty. \tag{9}$$

Using the condition $u = u_\infty(x) \rightarrow U_\infty x$ as $y \rightarrow \infty$ in Eq. (4) gives

$$u \frac{\partial u}{\partial x} + v \frac{\partial u}{\partial y} = U_\infty \frac{du_\infty}{dx} + \nu \frac{\partial^2 u}{\partial y^2} + \frac{\nu}{\zeta} U_\infty x - \frac{\nu}{\zeta} u. \tag{10}$$

or

$$u \frac{\partial u}{\partial x} + v \frac{\partial u}{\partial y} = U_\infty \frac{du_\infty}{dx} + \nu \frac{\partial^2 u}{\partial y^2} + \frac{\nu}{\zeta} (U_\infty x - u). \tag{11}$$

With the help of RA [15], the heat flux due to radiation is given as

$$q_r = -\frac{4\sigma^*}{3k^*} \frac{\partial \theta^4}{\partial y}, \tag{12}$$

Utilizing Eq. (12), Eq. (5) transforms into the form:

$$u \frac{\partial \theta}{\partial x} + v \frac{\partial \theta}{\partial y} = \left(\frac{k}{\rho C_p} + \frac{16\sigma^* \theta_\infty^3}{3\rho C_p k^*} \right) \frac{\partial^2 \theta}{\partial y^2}. \tag{13}$$

For the above equation, the temperature difference is supposed to be low sufficiently within the flow which leads to the linearization of θ^4 as

$$\theta^4 \cong 4\theta_\infty^3 \theta - 3\theta_\infty^4$$

via Taylors series about θ_∞ and neglecting higher terms. Equation (13) represents the flow equation of temperature with linear TR. But the present problem aims to explore

the influence of nonlinear TR on the flow, so neglecting the above supposition, i.e. replacement of θ_∞^3 with θ^3 in Eq. (12) and then putting it in Eq. (5) gives [34, 44].

$$u \frac{\partial \theta}{\partial x} + v \frac{\partial \theta}{\partial y} = \frac{k}{\rho C_p} \frac{\partial}{\partial y} \left(\left(1 + \frac{16\sigma^* \theta^3}{3kk^*} \right) \frac{\partial \theta}{\partial y} \right). \tag{14}$$

Now, introducing the similarity transformations and non-dimensional temperature and concentrations.

$$\psi = (U_\infty v)^{\frac{1}{2}} x f(\eta), \Theta(\eta) = \frac{\theta - \theta_\infty}{\theta_w - \theta_\infty}, \phi_1(\eta) = \frac{c}{c_o}, \tag{15}$$

$$\phi_2(\eta) = \frac{d}{c_o}, \eta = \left(\frac{U_\infty}{v} \right)^{\frac{1}{2}} y$$

The following normalized form of Eqs. (11), (14), (6) and (7) is achieved after using Eq. (15):

$$f''' - f'^2 + ff'' + 1 + \beta(1 - f') = 0, \tag{16}$$

$$\left(\left(1 + Rd(1 + (\Theta_w - 1)\Theta)^3 \right) \Theta' \right)' + Pr f \Theta' = 0, \tag{17}$$

$$\frac{1}{Sc_C} \phi_1'' + f \phi_1' - K \phi_1 \phi_2^2 = 0, \tag{18}$$

$$\frac{\delta}{Sc_D} \phi_2'' + f \phi_2' + K \phi_1 \phi_2^2 = 0. \tag{19}$$

Here $\beta = \frac{v}{\zeta U_\infty}$, $\Theta_w = \frac{\theta_w}{\theta_\infty}$, $Rd = \frac{16\sigma^*}{3kk^*}$, $Sc_C = \frac{v}{D_c^*}$, $Sc_D = \frac{v}{D_d^*}$, $K = \frac{k_c c_o^2}{U_\infty}$ and $Pr = \frac{v}{\alpha}$.

The surface constraints (8) and (9) become

$$\begin{aligned} f(0) = 0, f'(0) = \lambda, \Theta(0) = 1, \\ \phi_1'(0) = K_s \phi_1(0), \delta \phi_2'(0) = -K_s \phi_1(0), \end{aligned} \tag{20}$$

$$\left. \begin{aligned} f'(\eta) = 1, \Theta(\eta) \rightarrow 0, \\ \phi_1(\eta) \rightarrow 1, \phi_2(\eta) \rightarrow 0 \end{aligned} \right\} \text{ as } \eta \rightarrow \infty. \tag{21}$$

Here $\lambda = \frac{U_w}{U_\infty}$, $K_s = \frac{k_s}{Re^{1/2} D_c^*}$, $\delta = \frac{D_d^*}{D_c^*}$.

3 Numerical Solution

Shooting technique with the aid of Runge–Kutta algorithm is adopted to solve the two-point boundary value problem generated by nonlinear ordinary DEs (16)–(19) along with surface constraints (20)–(21). First, the problem is transformed into an initial value problem (IVP) as

$$\left. \begin{aligned} f' &= \xi_1, \\ f'' &= \xi_2, \\ \xi_2' &= \xi_1^2 - f \xi_2 - 1 - \beta(1 - \xi_1). \end{aligned} \right\} \tag{22}$$

$$\left. \begin{aligned} \Theta &= \zeta_1, \\ \zeta_1' &= \zeta_2, \\ \zeta_2' &= \frac{Pr f \zeta_2 - 3Rd(\Theta_w - 1)\zeta_2^2(1 + (\Theta_w - 1)\zeta_1)^2}{1 + Rd(1 + (\Theta_w - 1)\zeta_1)}. \end{aligned} \right\} \tag{23}$$

$$\left. \begin{aligned} \phi_1 &= \Psi_1, \\ \Psi_1' &= \Psi_2, \\ \Psi_2' &= Sc_C(K\Psi_1\Psi_1^2 - f\Psi_1). \end{aligned} \right\} \tag{24}$$

and

$$\left. \begin{aligned} \phi_2 &= \Phi_1, \\ \Phi_1' &= \Phi_2, \\ \Phi_2' &= \frac{Sc_D}{\delta}(-K\Psi_1\Phi_1^2 - f\Phi_2), \end{aligned} \right\} \tag{25}$$

with the constraints

$$\begin{aligned} f(0) = 0, \quad \zeta_1(0) = \lambda, \quad \Psi_1(0) = (1/K_s)\Psi_2(0), \\ \Phi_2(0) = -(K_s/\delta)\Psi_1(0). \end{aligned} \tag{26}$$

The appropriate value of the finite value of $\eta \rightarrow \infty$ say η_∞ has a vital role in this method. To solve Eqs. (22)–(25) subject to conditions (26) as an IVP, values for $\xi_2(0)$ i.e. $f''(0)$, $\zeta_2(0)$ i.e. $\theta'(0)$, $\Psi_2(0)$ i.e. $\phi_1'(0)$ and $\Phi_1(0)$ i.e. $\phi_2(0)$ are required, but the problem does not have such values. After selecting the initial guesses for $\xi_2(0)$, $\zeta_2(0)$, $\Psi_2(0)$, $\Phi_1(0)$ and employing the Runge–Kutta method, the solution is obtained. The better approximation of the solution is achieved by adjusting the values for $\xi_2(0)$, $\zeta_2(0)$, $\Psi_2(0)$ and $\Phi_1(0)$. For this, Newton’s approach has been used.

4 Results and Discussion

A numerical technique, namely shooting procedure, is opted to find the solution of the flow equations for the flow near SP in the presence of generalized TR and porous zone. The unequal diffusivities of two reactive species are also considered for the concentration profile. Graphs are presented to examine the response of velocity $f'(\eta)$, temperature $\Theta(\eta)$, and concentrations $\phi_1(\eta)$, $\phi_2(\eta)$ to the change in the governing parameters, i.e. λ , β , Rd , Pr , Θ_w , δ , K_s , K , Sc_C and Sc_D arising in the flow equations.

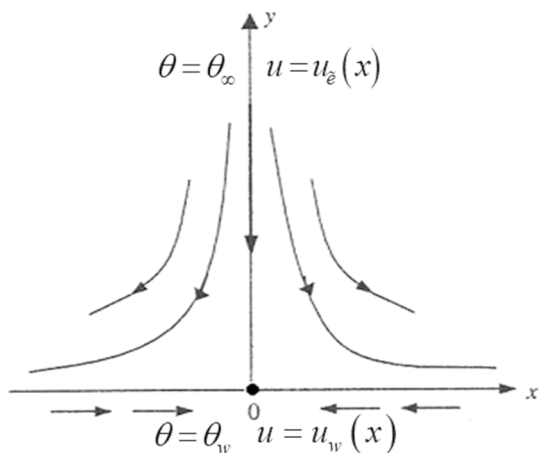


Fig. 1 Schematic of the problem

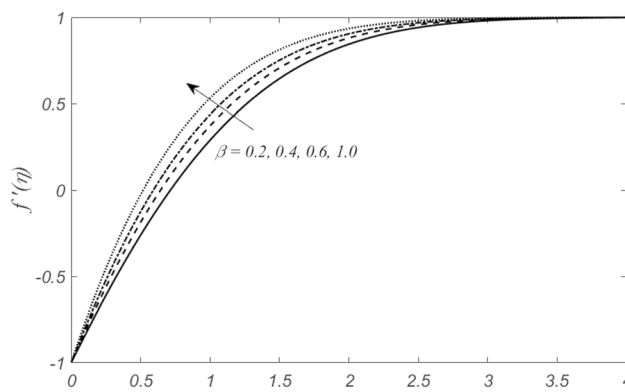


Fig. 3 Variation in $f'(\eta)$ with β when $\lambda = -1, Pr = 0.72, \Theta_w = 1.01, Rd = 1, Sc_C = Sc_D = 0.8, \delta = 1.2, K = 1$ and $K_s = 1$

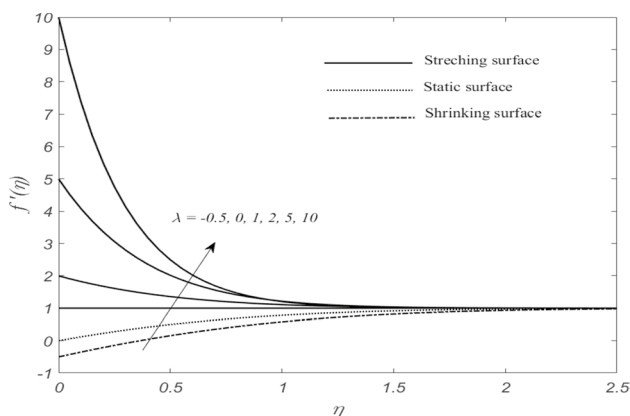


Fig. 2 Variation in $f'(\eta)$ with λ when $\beta = 0.06, Pr = 0.72, \Theta_w = 1.01, Rd = 1, Sc_C = Sc_D = 0.8, \delta = 1.2, K = 1$ and $K_s = 1$

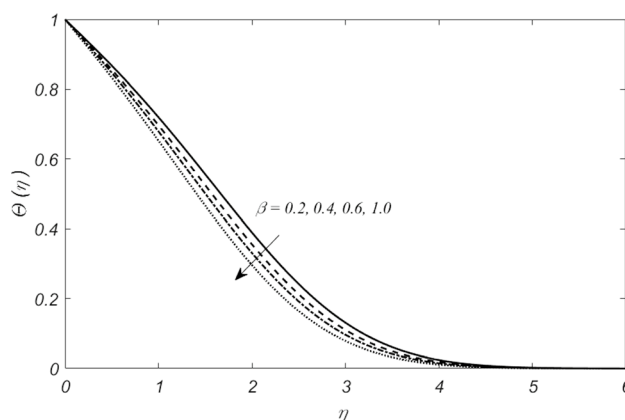


Fig. 4 Variation in $\Theta(\eta)$ with β when $\lambda = -1, Pr = 1.5, \Theta_w = 1.01, Rd = 1, Sc_C = Sc_D = 0.8, \delta = 1.2, K = 1$ and $K_s = 1$

Figure 2 shows the deviation in $f'(\eta)$ for various values of the SS parameter λ . $\lambda < 0$ means the shrinking of the surface, $\lambda = 0$ symbolizes the static surface while $\lambda > 0$ stands for stretching of the surface. From figure, it can be viewed that $f'(\eta)$ increases with an increase in λ . However, the BL thickness for the shrinking surface is more significant than static and stretched surfaces. Figure 3 is graphed to show the behavioural change in $f'(\eta)$ with an increment in β when the flow is over a shrinking wall. A decrease in the BL region is observed with a rise in the permeability of the porous zone. This reduction is related to Darcy's resistance which enhances with the increase in β .

Figures 4, 5, 6, and 7 are plotted to present the influence of evolving parameters on the temperature profile $\Theta(\eta)$. Figure 4 illustrates the effects of β on $\Theta(\eta)$ over a shrinking wall. It can be seen that $\Theta(\eta)$ as well as thermal BL is a decreasing function of β . Fig. 5 depicts the change in $\Theta(\eta)$ with an increase in Θ_w . It can be noticed that both thermal

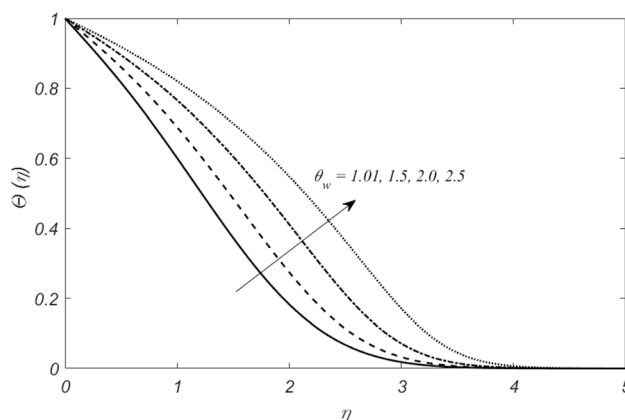


Fig. 5 Variation in $\Theta(\eta)$ with Θ_w when $\lambda = -1, \beta = 1, Pr = 0.72, Rd = 1, Sc_C = Sc_D = 0.8, \delta = 1.2, K = 1$ and $K_s = 1$

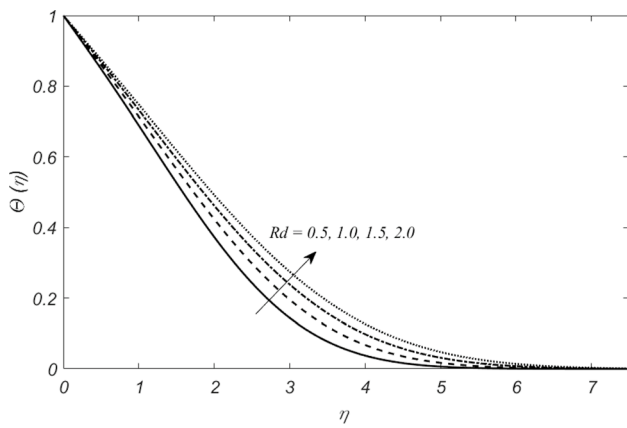


Fig. 6 Variation in $\Theta(\eta)$ with Rd when $\lambda = -1, \beta = 1, Pr = 0.72, \Theta_w = 1.01, Sc_C = Sc_D = 0.8, \delta = 1.2, K = 1$ and $K_s = 1$

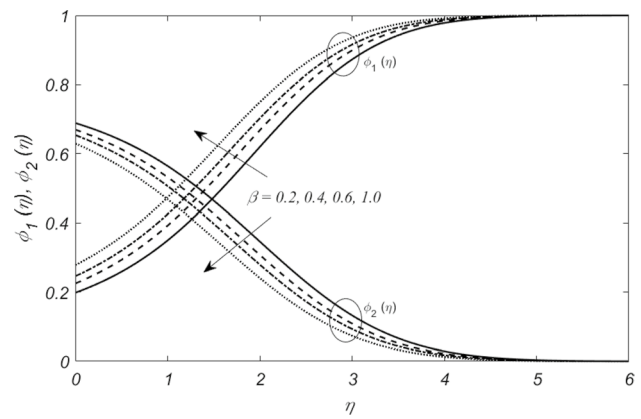


Fig. 8 Variation in $\phi_1(\eta), \phi_2(\eta)$ with β when $\lambda = -1, Pr = 0.72, \Theta_w = 1.01, Rd = 1, \delta = 1.1, Sc_C = Sc_D = 0.6, K = 0.9$ and $K_s = 0.9$

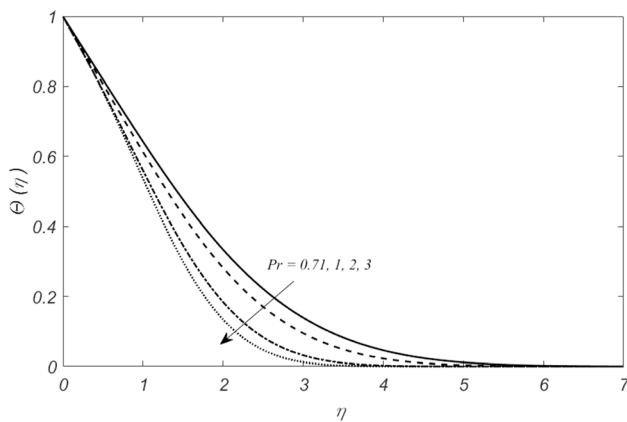


Fig. 7 Variation in $\Theta(\eta)$ with Pr when $\lambda = -1, \beta = 1, Rd = 1, \Theta_w = 1.01, Sc_C = Sc_D = 0.8, \delta = 1.2, K = 1$ and $K_s = 1$

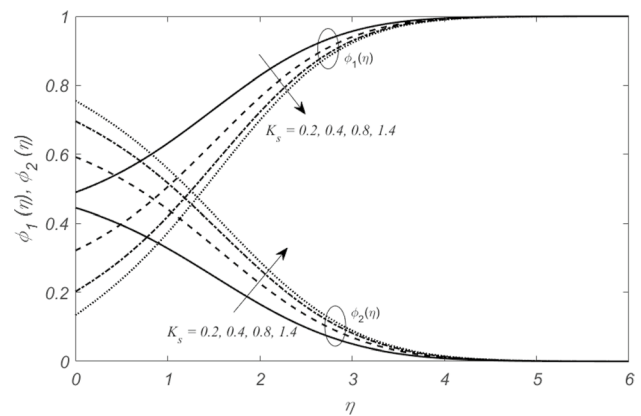


Fig. 9 Variation in $\phi_1(\eta), \phi_2(\eta)$ with K_s when $\lambda = -1, Pr = 0.72, \Theta_w = 1.01, Rd = 1, \delta = 1.2, Sc_C = Sc_D = 0.8, K = 1$ and $\beta = 1$

BL and $\Theta(\eta)$ enhance with a raise in θ_w . The change in $\Theta(\eta)$ with the increasing values of Rd can be observed from Fig. 6 which depicts a rise in both $\Theta(\eta)$ and its BL region with raise in Rd . The decreasing effect of Pr on $\Theta(\eta)$ can be noticed in Fig. 7. The decrease in thermal BL is also seen in this Figure.

The impacts of ruling parameters on the concentration profiles $\phi_1(\eta), \phi_2(\eta)$ are shown in Figs. 8, 9, 10, 11, 12. Figure 8 presents the change in the behaviour of $\phi_1(\eta), \phi_2(\eta)$ with an increment in β . A decrement in the regions of BL for both $\phi_1(\eta)$ and $\phi_2(\eta)$ is observed from this Figure with an increase in β due to porosity resistance. However, $\phi_1(\eta)$ is showing an increment and $\phi_2(\eta)$ is decreasing with a rise in β . The response of $\phi_1(\eta), \phi_2(\eta)$ with a hike in the values of K_s is portrayed in Fig. 9. The effect of K_s on concentration BL is reverse of β , i.e. for both $\phi_1(\eta)$ and $\phi_2(\eta)$ BL increases with a raise in K_s . Figure also shows

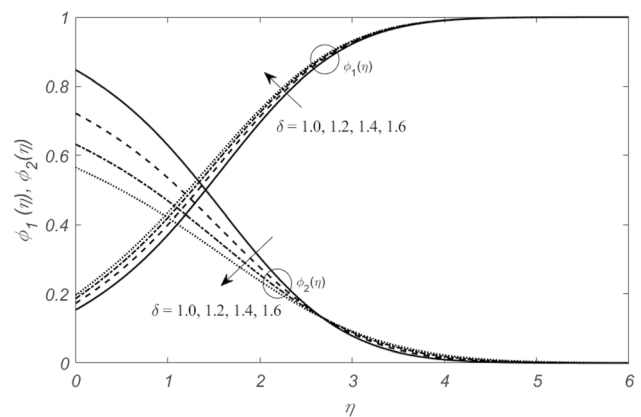


Fig. 10 Variation in $\phi_1(\eta), \phi_2(\eta)$ with δ when $\lambda = -1, Pr = 0.72, \Theta_w = 1.01, Rd = 1, \beta = 1, Sc_C = Sc_D = 0.8, K = 1$ and $K_s = 1$

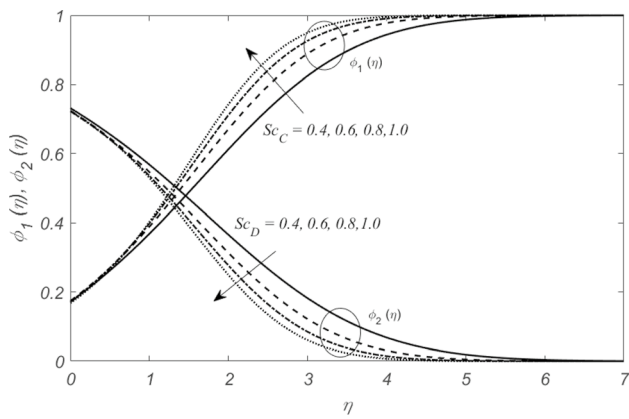


Fig. 11 Variation in $\phi_1(\eta), \phi_2(\eta)$ with Sc_C and Sc_D when $\lambda = -1, Pr = 0.72, \Theta_w = 1.01, Rd = 1, \beta = 1, \delta = 1.2, K = 1$ and $K_s = 1$

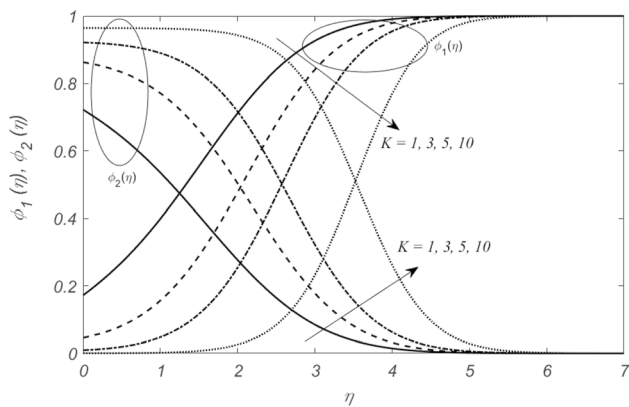


Fig. 12 Variation in $\phi_1(\eta), \phi_2(\eta)$ with K when $\lambda = -1, Pr = 0.72, \Theta_w = 1.01, Rd = 1, \beta = 1, Sc_C = Sc_D = 0.8, \delta = 1.2$ and $K_s = 1$

a reduction and an increment in $\phi_1(\eta)$ and $\phi_2(\eta)$, respectively. The varying behaviour of $\phi_1(\eta), \phi_2(\eta)$ with change in δ is graphed in Fig. 10. The response of $\phi_1(\eta)$ and $\phi_2(\eta)$ to the increase in δ is similar to that of β . However, the variance in $\phi_2(\eta)$ is greater relative to $\phi_1(\eta)$. Due to the rate of diffusion coefficient δ , the shift in the concentration profile is more notable in the concentration of species D relative to species C. A contraction in the BL region of both $\phi_1(\eta)$ and $\phi_2(\eta)$ with the increasing values of Sc_C and Sc_D is observed and can be seen in Fig. 11. The change Sc_C leads to an increase in $\phi_1(\eta)$ while the rise in Sc_D reduces $\phi_2(\eta)$. As a consequence of increasing Schmidt number, the mass diffusivity of the species decreases, thereby reducing the concentration BL thickness for both Sc_C and Sc_D . Figure 12 shows that the variation in both $\phi_1(\eta)$ and $\phi_2(\eta)$ for distinct values of K . The change in the BL region for K has similar behaviour to that K_s , i.e. the thickness region of

Table 1 Comparison of $f''(0)$ for a stretching sheet obtained for different values of λ , for fixed values of $\beta = 1$

λ	Shaw et al. [45]	Present
0	1.23258766	1.23258766
0.1	1.14656100	1.14656100
0.2	1.05112999	1.05112999
0.3	0.94681612	0.94681612
0.4	0.83407209	0.83407209
0.5	0.71329496	0.71329496
1	0	0
2	-1.88730667	-1.88730667
3	-4.276541	-4.276541
4	-7.086378	-7.086378
5	-10.264749	-10.264749

Table 2 Comparison of $f''(0)$ for a shrinking sheet obtained for different values of λ , for fixed values of $\beta = 1$

λ	Shaw et al. [45]		Present	
	$f_1''(0)$	$f_2''(0)$	$f_1''(0)$	$f_2''(0)$
-0.25	1.40224081	1.476217	1.40224081	1.476217
-0.5	1.49566977	-	1.49566977	-
-0.75	1.48929824	-	1.48929824	-
-1	1.32881688	-	1.32881688	-
-1.05	1.26622764	0.01217792	1.26622764	0.01217792
-1.1	1.18668029	0.04922896	1.18668029	0.04922896
-1.15	1.08223117	0.11670214	1.08223117	0.11670214
-1.2	0.93247336	0.23364973	0.93247336	0.23364973
-1.2465	0.58428167	0.55429620	0.58428167	0.55429620

concentration boundary layer increases when K and K_s are increased, and it is because of reactants of different reactions of species. However, $\phi_1(\eta)$ reduces for larger values of K and the curve takes a S shape as K increases. An opposite trend is noticed for $\phi_2(\eta)$.

The comparison of the numerical values of $f''(0)$ with the findings stated by Shaw et al. [45] for the different values of λ are shown in Table 1 and 2 and found in excellent accordance. For $\lambda > 0$ (stretching sheet), a solution for all values of λ can be accomplished whereas the solution for $\lambda < 0$ (shrinking sheet) occurs only in the region $\lambda \geq \lambda_c = -1.2465$, here λ_c denotes the critical value of λ so that for $\lambda < \lambda_c$ no solution exist. However, for $\lambda_c < \lambda < -1$, the solution is not unique, so there exist two solutions $f_1(\eta)$ and $f_2(\eta)$. One can see from the literature that the first solution is stable and technically feasible, although the second solution is not.

5 Concluding Remarks

The impact of HH reactions on steady BL flow due to the SS surface close to the SP through a porous medium in the presence of nonlinear TR is investigated. By using the shooting method, a numerical solution is obtained. The following remarks have been made:

- Porous media acts as a source of resistance in a flow; therefore, an increase in permeability parameter β causes a decrement in velocity, temperature and concentration BL thickness.
- Prandtl number decreases the temperature BL thickness because the increment in Prandtl number Pr causes decrement in the thermal diffusivity while BL thickness increases with Rd .
- When the magnitude of Θ_w is small, the decrease in temperature distribution from the wall to the free stream is marginal compared to the maximum decreasing trend when the magnitude of Θ_w is high.
- As a result of rising values of Schmidt number, the mass diffusivity of the species decreases consequently both Sc_C and Sc_D reduce the concentration BL thickness.
- The increase in the magnitude of the ratio of diffusion coefficient is just a growing function of the catalyst concentration within the realm of fluid
- Both homogeneous and heterogeneous intensities increase concentration BL thickness.
- The results will be used in studies related to food processing, fog production and diffusion, highly acidic water bodies, chemical management equipment design, photocatalytic reactors, moisture over agricultural areas and fruit tree meadows, highly acidic water bodies, heat exchangers for fluidized beds.

Acknowledgements We are thankful to the reviewers for their encouraging comments and constructive suggestions to improve the quality of the manuscript.

References

1. Crane, L.J.: Flow past a stretching plate. *Zeitschrift Für Angewandte Mathematik und Physik ZAMP* **21**, 645–647 (1970). <https://doi.org/10.1007/BF01587695>
2. Parhi, S.; Nath, G.: Stability of viscous flow over a stretching sheet. *Acta Technica CSAV Ceskoslovensk Akad Ved* **34**, 389–409 (1989)
3. Kumaran, V.; Kumar, A.V.; Pop, I.: Transition of boundary layer flow past a stretching sheet due to a step change in applied constant mass flux. *Acta Mech.* **216**, 139–145 (2011). <https://doi.org/10.1007/s00707-010-0340-7>
4. Yirga, Y.; Tesfay, D.: Magnetohydrodynamic flow of viscous fluid over a non-linearly stretching sheet. *Open Access Libr. J.* **01**, 1–11 (2014). <https://doi.org/10.4236/oalib.1101030>
5. Hassan, H.S.: Symmetry analysis for MHD viscous flow and heat transfer over a stretching sheet. *Appl. Math.* **06**, 78–94 (2015). <https://doi.org/10.4236/am.2015.61009>
6. Sheikh, M.; Abbas, Z.: Effects of thermophoresis and heat generation/absorption on MHD flow due to an oscillatory stretching sheet with chemically reactive species. *J. Magn. Magn. Mater.* **396**, 204–213 (2015). <https://doi.org/10.1016/j.jmmm.2015.08.011>
7. Singh, J.; Mahabaleshwar, U.S.; Bognár, G.: Mass transpiration in nonlinear MHD flow due to porous stretching sheet. *Sci. Rep.* **9**, 1–15 (2019). <https://doi.org/10.1038/s41598-019-52597-5>
8. Polu, B.A.R.; Reddy, S.S.R.: Impact of thermal radiation and viscous dissipation on hydromagnetic unsteady flow over an exponentially inclined preamable stretching sheet. *J. Comput. Appl. Res. Mech. Eng.* (2019). <https://doi.org/10.22061/jcarm.2019.3709.1433>
9. Wang, C.Y.: Stagnation flow towards a shrinking sheet. *Int. J. Non-Linear Mech.* **43**, 377–382 (2008). <https://doi.org/10.1016/j.ijnonlinmec.2007.12.021>
10. Lok, Y.Y.; Ishak, A.; Pop, I.: MHD stagnation-point flow towards a shrinking sheet. *Int. J. Numer. Methods Heat Fluid Flow* **21**, 61–72 (2011). <https://doi.org/10.1108/09615531111095076>
11. Rosali, H.; Ishak, A.: Stagnation-point flow over a stretching/shrinking sheet in a porous medium. *AIP Conf. Proc.* **1571**, 949–955 (2013). <https://doi.org/10.1063/1.4858776>
12. Yasin, M.H.M.; Ishak, A.; Pop, I.: MHD stagnation-point flow and heat transfer with effects of viscous dissipation, joule heating and partial velocity slip. *Sci. Rep.* **5**, 1–8 (2015). <https://doi.org/10.1038/srep17848>
13. Nasir, N.A.A.M.; Ishak, A.; Pop, I.; Zainuddin, N.: MHD stagnation point flow towards a quadratically stretching/shrinking surface. *J. Phys. Conf. Ser.* (2019). <https://doi.org/10.1088/1742-6596/1366/1/012013>
14. Alarifi, I.M.; Abokhalil, A.G.; Osman, M.; Lund, L.A.; Ayed, M.B.; Belmabrouk, H.; Iskander, T.: MHD flow and heat transfer over vertical stretching sheet with heat sink or source effect. *Sym. Basel* (2019). <https://doi.org/10.3390/sym11030297>
15. Magyari, E.; Pantokratoras, A.: Note on the effect of thermal radiation in the linearized Rosseland approximation on the heat transfer characteristics of various boundary layer flows. *Int. Commun. Heat Mass Trans.* **38**, 554–556 (2011). <https://doi.org/10.1016/j.icheatmasstransfer.2011.03.006>
16. Pantokratoras, A.: Natural convection along a vertical isothermal plate with linear and non-linear Rosseland thermal radiation. *Int. J. Thermal Sci.* **84**, 151–157 (2014). <https://doi.org/10.1016/j.ijthe.2014.05.015>
17. Laxmi, T.V.; Shankar, B.: Effect of nonlinear thermal radiation on boundary layer flow of viscous fluid over nonlinear stretching sheet with injection/suction. *J. Appl. Math. Phys.* **04**, 307–319 (2016). <https://doi.org/10.4236/jamp.2016.42038>
18. Waqas, H.; Khan, S.U.; Bhatti, M.M.; Imran, M.: Significance of bioconvection in chemical reactive flow of magnetized Carreau–Yasuda nanofluid with thermal radiation and second-order slip. *J. Thermal Anal. Calor.* **140**(3), 1293–1306 (2020)
19. Riaz, A.; Ellahi, R.; Bhatti, M.M.; Marin, M.: Study of heat and mass transfer in the Eyring–Powell model of fluid propagating peristaltically through a rectangular compliant channel. *Heat Transf. Res.* **50**(16), 1539–1560 (2019)
20. Hashim, I.; Sardar, H.; Khan, M.: Mixed convection flow and heat transfer mechanism for non-Newtonian Carreau nanofluids under the effect of infinite shear rate viscosity. *Phys. Scr.* **95**, 035225 (2020). <https://doi.org/10.1088/1402-4896/AB41E9>
21. Pattnaik, P.K.; Mishra, S.; Bhatti, M.M.: Duan–Rach approach to study ethylene glycol C2H6O2 nanofluid flow based upon model. *Inventions* **5**(3), 1–23 (2020)
22. Zhang, L.; Arain, M.B.; Bhatti, M.M.; Zeeshan, A.; Hal-Sulami, H.: Effects of magnetic Reynolds number on swimming of



- gyrotactic microorganisms between rotating circular plates filled with nanofluids. *Appl. Math. Mech.* **41**(4), 637–654 (2020)
23. Chaudhary, M.A.; Merkin, J.H.: A simple isothermal model for homogeneous-heterogeneous reactions in boundary-layer flow. I Equal diffusivities. *Fluid Dyn. Res.* **16**, 311–333 (1995). [https://doi.org/10.1016/0169-5983\(95\)00015-6](https://doi.org/10.1016/0169-5983(95)00015-6)
 24. Chaudhary, M.A.; Merkin, J.H.: stretchingshrinking sheet with uniform suction and slip effects. *Fluid Dyn. Res.* **16**, 335–359 (1995). [https://doi.org/10.1016/0169-5983\(95\)90813-H](https://doi.org/10.1016/0169-5983(95)90813-H)
 25. Animasaun, I. L.; Raju, C. S. K.; Sandeep, N.; Unequal diffusivities case of homogeneous–heterogeneous reactions within viscoelastic fluid flow in the presence of induced magnetic-field and nonlinear thermal radiation. *Alexandria Eng. J.* **55**, 1595–1606 (2016)
 26. Sheikh, M.; Abbas, Z.: Homogeneous–heterogeneous reactions in stagnation point flow of Casson fluid due to a stretching/shrinking sheet with uniform suction and slip effects. *Ain Shams Eng. J.* (2017). <https://doi.org/10.1016/j.asej.2015.09.010>
 27. Alghamdi, M.: On magnetohydrodynamic flow of viscoelastic nanofluids with homo-geneous -heterogeneous reactions. *Coatings* (2020). <https://doi.org/10.3390/coatings10010055>
 28. Das, R.: Estimation of Radius Ratio in a Fin Using Inverse CFD Model. *CFD Lett.* **3**(1), 40–47 (2011)
 29. Das, R.: A simplex search method for a conductive–convective fin with variable conductivity. *Int. J. Heat Mass Transf.* **54**, 5001–5009 (2011)
 30. Das, R.: A simulated annealing-based inverse computational fluid dynamics model for unknown parameter estimation in fluid flow problem. *Int. J. Comput. Fluid Dyn.* **26**, 499–513 (2012). <https://doi.org/10.1080/10618562.2011.632375>
 31. Das, R.: Inverse analysis of Navier-Stokes equations using simplex search method. *Inverse Probl. Sci. Eng.* **20**(4), 445–462 (2012). <https://doi.org/10.1080/17415977.2011.629046>
 32. Das, R.: Three-Parameter estimation study in a radial fin geometry using FDM based simplex method. *Heat Transf. Eng.* **35**, 1309–1319 (2014). <https://doi.org/10.1080/01457632.2013.876866>
 33. Das, R.: Estimation of parameters in a fin with temperature-dependent thermal conductivity and radiation. *Proc. IMech. E Part E J. Process Mech. Eng.* **230**(6), 474–485 (2016)
 34. Rashad, A.; El-Hakiem, M.: Effect of radiation on non-darcy free convection from a vertical cylinder embedded in a fluid-saturated porous medium with a temperature-dependent viscosity. *J. Porous Media* **10**(2), 209–218 (2007)
 35. Rashad, A.; EL-Kabeir, S.: Heat and mass transfer in transient flow by mixed convection boundary layer over a stretching sheet embedded in a porous medium with chemically reactive species. *J. Porous Media* **13**, 75–85 (2010)
 36. El-Kabeir, S.; Chamkha, A.; Rashad, A.: Heat and mass transfer by MHD stagnation-point flow of a power-law fluid towards a stretching surface with radiation, chemical reaction and sores and dufour effects. *Int. J. Chem. React. Eng.* **8**, 1–18 (2010)
 37. Rashad, A.; Chamkha, A.; El-Kabeir, S.: Effect of chemical reaction on heat and mass transfer by mixed convection flow about a solid sphere in a saturated porous media. *Int. J. Numer. Methods Heat Fluid Flow* **21**(4), 418–433 (2011)
 38. Rashad, A.; Chamkha, A.; El-Kabeir, S.: Effects of radiation and chemical reaction on heat and mass transfer by natural convection in a micropolar fluid saturated porous medium with streamwise temperature and species concentration variations. *Heat Transf. Res.* **45**(8), 795–815 (2014)
 39. Chamkha, A.; Kabeir, S.M.M.; Rashad, A.: Unsteady coupled heat and mass transfer by mixed convection flow of a micropolar fluid near the stagnation point on a vertical surface in the presence of radiation and chemical reaction. *Progress Comput. Fluid Dyn.* **15**(3), 186–196 (2015)
 40. El-Kabeir, S.M.M.; Modather, M.; Rashad, A.: Heat and mass transfer by unsteady natural convection over a moving vertical plate embedded in a saturated porous medium with chemical reaction, sores and dufour effects. *J. Appl. Fluid Mech.* **8**(3), 453–463 (2015)
 41. Nabwey, H.A.; Kabeir, S.M.M.; Rashad, A.: Lie group analysis of effects of radiation and chemical reaction on heat and mass transfer by unsteady slip flow from a non-isothermal stretching sheet immersed in a porous medium. *J. Comput. Theor. Nanosci.* **12**(11), 4056–4062 (2015)
 42. Subbarayudu, K.; Suneetha, S.; Bala, A.R.; Rashad, A.M.: Framing the activation energy and binary chemical reaction on cnt's with cattaneo-christov heat diffusion on maxwell nanofluid in the presence of nonlinear thermal radiation. *Arabian J. Sci. Eng.* **44**, 10313–10325 (2019)
 43. Reddy, S.R.R.; Bala, A.R.P.; Rashad, A.M.: Activation energy impact on chemically reacting eyring-powell nanofluid flow over a stretching cylinder. *Arab. J. Sci. Eng.* **45**(7), 5227–5242 (2020)
 44. Souayeh, B.; Reddy, M.G.; Sreenivasulu, P.; Poornima, T.; Rahimi-Gorji, M.; Alari, I.M.: Comparative analysis on nonlinear radiative heat transfer on MHD Casson nano fluid past a thin needle. *J. Mol. Liquids* **284**, 163–174 (2019). <https://doi.org/10.1016/j.molliq.2019.03.151>
 45. Shaw, S.; Kameswaran, P. K.; Precious Sibanda, P.: Homogeneous-heterogeneous reactions in micropolar fluid flow from a permeable stretching or shrinking sheet in a porous medium. *Boundary Value Probl.* **2013**(77), (2013)

